ISSN 1330-3651 (Print), ISSN 1848-6339 (Online) https://doi.org/10.17559/TV-20230720000816
Original scientific paper

An Optimized Design Modeling of PV Integrated SEPIC Based Single-Phase System

Ravikumar SUDHANTHIRARAJAN*, Venkatanarayanan SUBARAMANIYAN

Abstract: Power converters are widely used in renewable energy conversion systems such as photovoltaics. Their main role is to adapt the output voltage to a desired voltage shape.This study proposes a highly efficient Single-Ended Primary Inductor Converter (SEPIC) to enhance the utilization of PV arrays by ensuring a continuous flow of current. To minimize DC voltage ripples, a Proportional-Integral (PI) controller is presented to continuously monitor the High power extracted from the PV array. The PI controller parameters are optimized using the Osprey Optimization Algorithm (OOA), which mimics the hunting behavior of ospreys in nature. The OOA draws inspiration from the hunting strategy of ospreys when they hunt fish in the seas. The osprey first detects the position of its prey and then captures it, carrying it to a suitable location to consume it. Similarly, the OOA iteratively optimizes the PI controller parameters to advance the SEPIC converter and achieve a DC-link voltage for steady-state at the converter's output. Then it is fed into a voltage source inverter (VSI), which connects the system to a single-phase utility grid. A fuzzy logic tuned PI controller is employed to synchronize the inverter's output with the grid. The performance is evaluated by analyzing the harmonic content in the grid current. To validate the proposed approach, a Simulink model is developed and compared against a hardware prototype. The proposed results achieved an effectiveness of performance and efficient power conversion in the system.

Keywords: osprey optimization algorithm; proportional - integral controller; PV system; single - ended primary inductor converter; voltage source inverter

1 INTRODUCTION

Recently, renewable energy resources are replenishing in almost all the fields of domestic as well as industrial applications. Successful integration of solar PV fed grid has been incessantly thriving but it has some impact on the production of electricity [1-3]. SEPIC is utilized broadly for better execution of change of voltage Some uses of converter just need to buck/boost the voltage and can basically utilize the relating to input in some cases the yield are not as indicated by input. At that point all things considered, it is typically utilize best to convert that can diminish or expand the voltage Buck-Boost is less expensive yet they heat up and having just a capacitor and inductor which causes high measure of info current wave and this will make high measure of harmonics and its cure is costly and consequently this makes buck-boost converter pricey segment as well. PV energy systems offer a promising solution as they provide non-polluting, sustainable, and safe electricity [4]. Recent advancements in PV technology have led to increased module efficiency and decreased prices. While PV systems are cost-effective where natural gas power plants or wind farms are more cheap[5]. Therefore, further research is needed to improve the PV system penetration rate and enhance their economic viability.

The economic feasibility of PV systems is directly related to the amount of power from PV modules. Hence, it is imperative to focus on research studies aimed at maximizing power extraction from PV modules. These studies can explore various approaches, such as advanced optimization algorithms, improved system design, and enhanced energy conversion techniques. By increasing the efficiency and performance of PV systems, we can accelerate the transition to clean and sustainable energy sources, ultimately mitigating the negative impacts of greenhouse gas emissions.

Partial shading can have an important power impact output of a PV system, leading to a sharp decrease in power generation and instability in the output voltage. There is a need for a versatile power conversion system that can efficiently adjust the variable or fixed input DC voltage to the required value, especially in the context of solar energy. While conventional converters such as Boost, Buck or Buck-Boost configurations have been widely used, they come with significant drawbacks [5-8]. These include pulsating input and output power, high switching losses, fabrication costs, and rating restrictions. To overcome these limitations, advanced power converters have been developed to minimize ripple effects. Among these converters, the Cuk Converter, pioneered by Slobodan Cuk, stands out due to its unique ability to maintain continuous input and output currents and operate in both buck and boost modes by adjusting the duty cycle of a single switch in the circuit. It also features an inverted output characteristic that distinguishes it from other converters. However, both converters can impose high electrical stress on the components, potentially leading to component malfunction or overheating. SEPIC converters offer a solution to address these challenges. They provide a non-inverted output, which ensures uninterrupted and precise input for the circuits.

To ensure a PV's stable operation, proposed SEPIC controllers are employed. However, the previous method relies on sliding mode and hysteresis controllers, that encounter challenges in accurately tracking time-varying surfaces [9, 10]. In the current system, a PI controller is presented to maintain a constant power [11]. However, the PI controller relies on a trial-and-error approach, which may not optimize the control performance effectively. Moreover, the maximum power point tracking (MPPT) using the PI controller minimises ripples present in the DC voltage as required. As a result, there is a need for an improved control strategy that can address these limitations and ensure better control performance in the PV system. This work is used to improve the utilization of PV arrays by ensuring a steady flow of current. To avoid a DC voltage ripples, a PI controller is implemented to continuously monitor and regulate the MPPT extracted from the PV array. To optimize the performance of the PI controller, the OOA is presented to estimate an optimal value of PI controller parameters to stable DC voltage output of SEPIC controller.

2 RELATED WORKS

Several researchers have made significant contributions to the field of photovoltaic (PV) systems and their power electronics converters. M. Veerachary et al. [12] developed a V2-based MPPT scheme by buck-boost topology. However, for experimentation purposes, they chose to utilize a SEPIC converter based on coupled inductor concept for rippleless array current. This approach reduced magnetic core requirements and improved converter performance. M. Killi et al. [13] presented an adaptive voltage-sensor-based MPPT algorithm that utilizes a variable scaling factor for SEPIC. By adjusting the scaling factor, both steady-state and transient performance are increased to fix and adapt step size respectively.

In [14], the author A. R. Paul et al. proposed a SEPIC-Ćuk based transformer-less micro-inverter that has 1-high frequency switch and 4-line frequency switches; the circuit reduced losses in switching and enhanced system reliability. S. J. Chiang et al. [15] focused on PV charger with a SEPIC converter modelling. It is determined by both the PV module MPPT control loop and the battery charging loop. E. Mamarelis et al [16] proposed a sliding-mode controller design procedure for MPPT in PV applications. Their approach was applied to a SEPIC converter that can be extended to other suitable converters for PV applications. A fuzzy logic controller (FLC)-based SEPIC converter for MPPT operation is developed by A. Elkhateb et al. [17]. The proposed FLC utilized a convergent distribution of membership functions, resulting in faster response, reduced steady-state error, and small overshoot during variable-load scenarios.

T. K. Soon et al. [18] introduced an enhanced global search space differential evolution for MPPT in a PV system. Their algorithm demonstrated enhanced capability in MPPT, faster response to load variation, and easy tuning with fewer parameters to be set. A. Darwish et al [19] investigated three-phase differential-mode buck-boost inverters. This method can eliminate an input third-order harmonic current and output second-order harmonic currents. K. S. Tey et al. [20] developed an enhanced DC-DC converter based on a hybrid SEPIC and CUK converters. This converter utilized a single switch and provided bipolar outputs, enabling power transfer to the grid. Integrated magnetics cores were used to reduce input current ripple and improve power extraction from the solar PV system.

A. K. Singh et al. [21] explored a multifunctional power electronic converter (PEC) with PV and grid. It accommodated vehicle modes such as charging, propulsion and regenerative braking effectively. K. K. Mohammed et al. [22] introduced an improved Rat Swarm Optimizer algorithm (IRSO) for MPPT. It was presented to improve the convergence speed towards the MPPT. It also developed a new approach to maintain a speed response for any DC-DC converter. S. Hasanpour et al. [23] proposed a single-switch trans-inverse high step-up suitable converter. It achieved low voltage stress and high voltage gains across the MOSFET, reducing the required conduction losses and duty cycle.

Several strategies for overcoming the power control issue were described, including P&O, fuzzy inference, genetic algorithm-based Perturb and Observe (P&O) and Particle Swarm Optimization (PSO). While the optimization strategies described above are suitable for nonlinear systems, the sophisticated computation and high delay time requirements considerably increase the controller's effort [24]. While a single stage voltage source converter (VSC) can be used to connect the solar array to the utility grid, the circuit complexity and presence of higher order harmonics make two-stage power conversion the preferable alternative. Due to its simplicity and greater availability, the conventional VSI (voltage source inverter) is the primary interface device in two-stage grid-connected photovoltaic systems.

3 PROPOSED METHODOLOGY

Fig. 1 illustrates the grid-integrated PV system proposed in this study. The primary objective established a seamless connection that ensures a stable voltage gain.

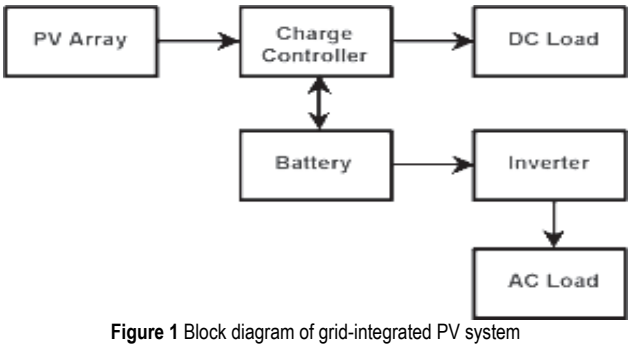

Figure 1 Block diagram of grid-integrated PV system

The system consists of a SEPIC converter with PV that is controlled by an optimized PI controller in single voltage sensor. A 1-phase voltage source inverter (VSI) and an LC filter are connected an output to the grid. Since the PV array voltage fluctuates due to changes in temperature and irradiation, the SEPIC converter consisting of two inductors and two capacitors, acts as a filter to reduce ripples in voltage. For DC voltage stability, an Osprey optimization-based PI controller is employed. This controller automatically updates its variables, ensuring a constant voltage value. The stabilized voltage is then fed to the 1-phase grid-connected inverter. The actual power grid serves as a PI reference controller, which generates control signals for inverter. It converts the DC quantity into pulsating AC voltage. However, the grid voltage and current can be impacted by distortions of harmonic introduced by nonlinear loads. The actual voltage and current evaluated inverter's output with minimum synchronization and harmonics grid.

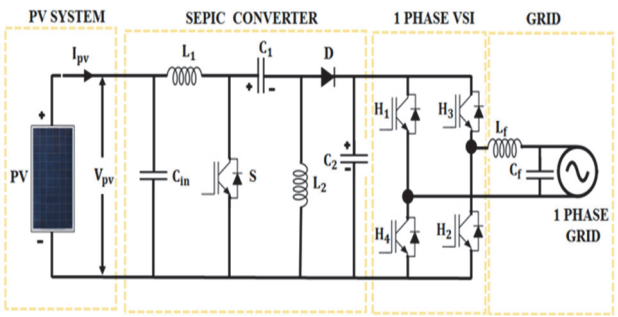

Figure 2 Circuit diagram of proposed system

This performance brings the voltage of grid as stable and synchronizes it with inverter's reference voltage. To maintain this stable state, fuzzy logic combined with a PI controller is used for grid synchronization. The proposed system's manipulating methods and structural framework effectively reduce the output ripple and maintain stability. Fig. 2 shows the circuit diagram.

3.1 PV Modelling

The uivalent circuit of diode is an important representation that helps in understanding the behavior and characteristics of the module. It provides insights into the relationship between the module's output current and voltage for various operating conditions.

In this work, a systematic controller-based high-gain SEPIC converter is utilized to enhance the PV's output power. The SEPIC converter is a type of DC-DC namely input/output isolation, high voltage gain, and efficient power conversion.

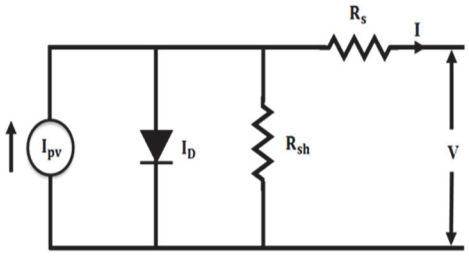

Figure 3 PV panel circuit

Eq. (1) describes the PV current flowing as:

$$I = I_{PV} - I_O \left[e^{\frac{(V+R_S I)}{V_k \alpha} - 1} \right] - \frac{V + IR_s}{R_{sh}} \tag{1}$$

where Io PV current's short circuit, V_k high Thermal Voltage, α ideality constant of Diode, I_{pv} PV Input current, I_d Diode Current, R_s Series Resistor, R_{sh} Shunt Resistor, I PV current output, V output Voltage of PV.

3.2 SEPIC Converter

It operates in two different modes such as continuous conduction mode (CCM) and discontinuous conduction mode (DCM). In the continuous conduction mode, the current flowing through the inductor never reaches zero during each switching cycle. This mode allows for smoother and continuous power transfer. On the other hand, in the discontinuous conduction mode, the inductor current drops to zero. This mode is suitable for applications with lighter load conditions. In Fig. 4, the SEPIC converter's circuit diagram is depicted, showcasing interconnections between various components. This circuit configuration allows for flexible voltage conversion capabilities, making it well-suited for applications where a wide range of input and output voltage levels are encountered.

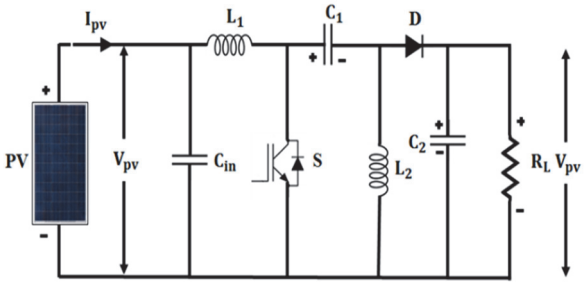

Figure 4 SEPIC converter

3.3 Mode 1

In the CCM of the SEPIC converter, the currents through the inductors L_1 and L_2 remain continuous and do not reach zero. As a result, these inductors are not completely discharged. Once the converter reaches a steady state, an input capacitor (C_{in}) becomes equal to the input voltage (V_{in}), resulting in no current flow through C_{in}. During this state, only inductor L_2 supplies the output current, and its average current is equal to the output current, regardless of V_{in}. In CCM, the cumulative average voltages across the inductors and capacitors (except C_s and C_o) are equal to the input voltage (V_{in}). This can be described by the following equation:

$$V_{in} = V_{L1} + VC_{in} + V_{L2} \tag{2}$$

Since the average voltage across C_{in} is equal to V_{in}, we can deduce that VL_1 is equal in magnitude but opposite in polarity to VL_2:

$$V_{L1} = -V_{L2} \tag{3}$$

When analyzing the SEPIC converter in CCM, it is essential to consider the conduction and non-conduction modes of the switch. In Fig. 5, the operation of the SEPIC converter during the conduction of switch S is illustrated. During the conduction mode, switch S is closed, allowing the current to flow through the inductor L and the input capacitor $C1$. At the same time, the diode D does not conduct which is reverse-biased and.

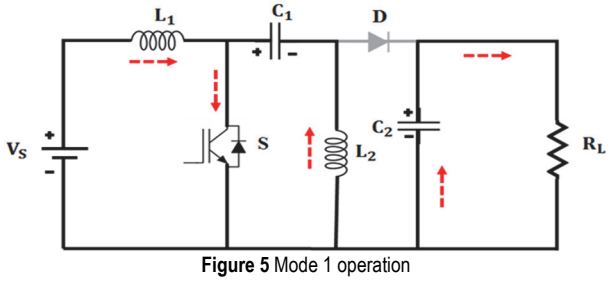

Figure 5 Mode 1 operation

The Vin is connected as series combination of L, C_1, and the load. The SEPIC converter in CCM operates by maintaining continuous current flow through the inductor, ensuring efficient energy transfer and voltage regulation.

3.4 Mode 2

In the discontinuous conduction mode (DCM), the switch S is opened, as depicted in Fig. 6. During this mode,

the input current flows through inductor L_1 and C in. Instantaneously current cannot change. The current in L_2 is discharged into capacitor C_2, causing diode D to turn on and supply current to the output. Though the S is open, both inductors contribute to the output current because their currents have the same direction. This allows for continuous power delivery to the load. The duty cycle (D) of the SEPIC converter can be calculated using Eq. (4). This duty cycle determines the energy transfer and voltage conversion characteristics of the SEPIC converter, allowing for precise control and regulation of the output voltage.

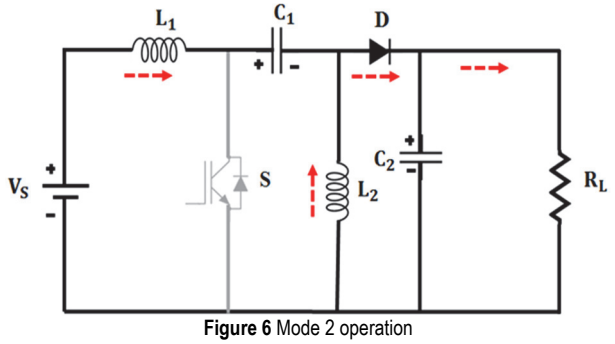

Figure 6 Mode 2 operation

$$Duty\ \ Cycle\ \ D = \frac{V_{OUT} + V_D}{V_{IN} + V_{AN} + V_D} \tag{4}$$

where V_{OUT} denotes Output Voltage, VD represents Diode Voltage, V_{IN} indicates Input Voltage

Both inductors and output capacitor C_2 can be determined using Eq. (5) and Eq. (6) respectively, whereas the load resistance (R) of the converter can be evaluated using Eq. (7), considering the output voltage and current.

$$L_1 = L_{2.3} = \frac{V_{\text{IN}} \times D_{\max}}{I_1 \times F_S} \tag{5}$$

$$C_2 = \frac{I_0 \times D_{\max}}{V_{\text{ripple}} \times V_D \times F_S} \tag{6}$$

I_o = Output Current, V_{ripple}= Ripple Voltage, $D_{\max}$ = Maximum value of diode, V_D = Diode Voltage, F_s = Switching frequency:

$$R = \frac{V_{\text{out}}}{I_{\text{out}}} \tag{7}$$

where V_{out} denotes an Output Voltage and I_{out} represents an Output Current.

The inductor current (ΔIL) can be estimated using Eq. (8), which takes into account the output current, output voltage, and a percentage (40%) of the input voltage.

$$\Delta IL = \frac{\text{I}_{\text{out}} \cdot V_o .40\%}{V_{\text{IN}}} \tag{8}$$

Finally, the voltage ripple across the coupling capacitor (C_1) can be determined using Eq. (9), which takes into account the output current, duty cycle ($D_{\max}$), and the capacitance value (C_1).

$$\Delta VC_1 = \frac{I_{\text{out}} \times D_{\max}}{C_1 \times F_S} \tag{9}$$

3.5 OOA

The concept of Osprey Optimization Algorithm (OOA) is derived from observing the hunting behavior of ospreys in nature. It is divided into two main phases: exploitation and exploration. These phases are implemented mathematically based on osprey's behavior during their hunting process. During the exploration phase, the algorithm explores the search space in a wide and diverse manner, similar to how ospreys scan the surroundings to locate potential prey. This phase focuses on discovering new solutions and expanding the search space to ensure a thorough exploration of the problem domain. The OOA's each osprey is determined and specified using Eq. (10).

$$FP_i = \left\{ X_k \,\middle|\, k \in \{1, 2, ..., N\} \wedge F_k < F_i \right\} \cup \{X_{\text{best}}\} \tag{10}$$

where FP_i is the fish locations for the I th osprey with best solution X_{best}.

New position of corresponding osprey is expressed using Eq. (11) and Eq. (13). If this new position leads to an improvement of an objective function, it replaces the osprey previous position based on Eq. (13).

$$x_{i,j}^{P1} = x_{i,j} + r_{i,j}\left(SF_{i,j} - I_{i,j} x_{i,j}\right) \tag{11}$$

$$x_{i,j}^{P1} = \begin{cases} x_{i,j}^{P1}, II_j \le x_{i,j}^{P1} \le ul_j \\ II_j, x_{i,j}^{P1} < Il_j \\ uI_j, x_{i,j}^{P1} \pm > ul_j \end{cases} \tag{12}$$

$$X_i = \begin{cases} X_i^{P1}, F_i^{P1} \le F_i \\ X_i, \text{else} \end{cases} \tag{13}$$

where, x_i^{P1} is the new location of prey and $x_{i,j}^{P1}$ is the jth dimension. r and I are the random numbers. Once the promising areas are identified during the exploration phase, osprey's approach catching and transporting the prey to a suitable location for consumption.

OOA based tuning.

The transfer function of the PI controller is given by Eq. (14).

$$G_c(s) = K_p + \frac{K_i}{s} \tag{14}$$

where K_p and K_i denote tuning parameters. The PI controller's output $u(t)$ is expressed in Eq. (15), which includes the proportional and integral terms.

$$u(t) = K_p e(t) + K_i \int_0^t e(t)\,dt \tag{15}$$

In this work, the Integral Absolute Error (IAE) is used as the performance index to evaluate the control objectives. The IAE, as defined in Eq. (16), represents the integral of the absolute error between an actual VDC and reference set point of SEPIC converter over time.

$$IAE = \int |e(t)|\,dt \tag{16}$$

The Kp and K_i values present an optimized using of the OOA algorithm.

Once the optimization process is completed, the tuned values of K_p and K_i obtained from the OOA algorithm are used in the PI controller. The PI controller generates a PWM reference signal, which is compared with a carrier signal to generate the PWM pulses. These PWM pulses are then applied to the SEPIC converter for controlling the output.

3.6 Grid Synchronization

Consider converter voltage (V_{dc}) as input that passed through a LPF to minimise ripples. The reference voltage (V_{dc}*) and filtered voltage are compared to evaluate a voltage error (Δv_{err}) for current sampling time, as given in Eq. (17).

$$\Delta V_{err}(n) = V_{dc}^{*}(n) V_{dc}(n) \tag{17}$$

A fuzzy-based PI controller is employed to modify the DC link voltage. The output current of the inverter (i_{inv}*) at the current sampling time is determined using Eq. (18), where K_{P1} denotes the proportional and K_{I1} represents an integral gain of the DC voltage controller, respectively.

$$\begin{aligned} i_{inv}^{*}(n) = i_{inv}^{*}(n-1) + K_{P1}\left(\Delta v_{err}(n) - \Delta v_{err}(n-1)\right) + \\ + K_{I1}\Delta v_{err}(n) \end{aligned} \tag{18}$$

The fuzzy-based PI controller tunes its parameters using fuzzy logic. Fuzzy logic allows for handling complex and imprecise information, enabling the controller to adapt to varying operating conditions. The tuning process involves defining fuzzy sets and membership functions to represent different control actions and their corresponding input/output relationships. The controller's rules are defined using linguistic variables and fuzzy IF-THEN statements, which map the input error (ΔV_{err}) to the output control action (i_{inv}*). The fuzzy-based PI controller adjusts the duty cycle (D) of the inverter by generating a modulation signal. This signal controls the inverter's operation and ensures that the output current meets the reference value.

4 RESULT AND DISCUSSION

The methodology of this study was implemented and analyzed using the MATLAB/SIMULINK software platform. Furthermore, experimental verification was conducted using the DSPIC30F2010 controller. The specifications for the solar panel, including the quantity of panels (3), the number of series-connected cells (36), the cell area (125 mm × 31.25 mm), the open circuit voltage (21.4 V), the optimal operating voltage (16.8 V), the short circuit current (1.21 A), the optimal operating current (1.19 A), the working temperature range (–40 °C to +85 °C), and the maximum system voltage (1000 V DC).

The simulation was conducted using established mathematical models of PV modules, charge controllers, and inverters. The degree of agreement or divergence between experimental and simulated outcomes was assessed by comparing key parameters such as power output, battery state of charge, and voltage-current characteristics. Any disparities between experimental and simulated results were analyzed to identify potential areas for improvement in the simulation model or the experimental setup.

The specifications for the SEPIC converter include the input voltage range (0 to 48V DC), the maximum input current (25 A), the capacitance values of C_1 and C_2 (20 uF), the inductance values of L_1 and L_2 (7 mH), and the output current (5 A). The main objective of this system is to ensure a stable power generation to the grid, regardless of variations in source voltage or load conditions. During daytime, the PV irradiance undergoes changes due to factors such as temperature and partial shading effects. The result achieved an irradiance level between 800 W/m^2 and 1000 W/m^2.

The proposed model is evaluated by analyzing the grid current and Total Harmonic Distortion (THD). The proposed results demonstrate the effectiveness in achieving improved current waveform quality and reduced THD. In the case of the traditional PI controller, the THD in the grid current is measured to be 3.41%. This indicates the presence of significant harmonic distortion in the current waveform, which can adversely affect the power quality and performance of connected electrical devices. However, with the proposed implementation, a remarkable improvement is observed. The THD in the grid current is significantly reduced to 1.8%. This indicates a substantial reduction in harmonic distortion, resulting in a cleaner and more sinusoidal current waveform.

4.1 Hardware Results

Fig. 12 provides hardware setup of the proposed syatem. The dsPIC30f2010 microcontroller, known for its reliable performance, has been successfully utilized to implement and develop the prototype of the proposed system.

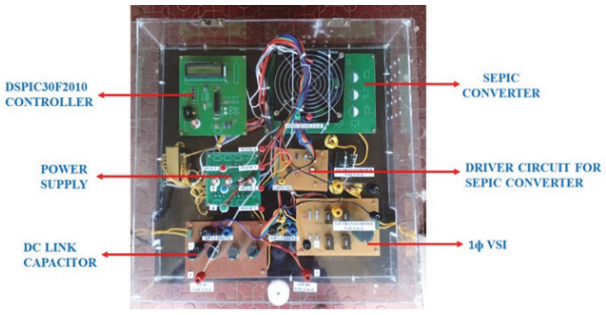

Figure 7 Hardware setup

Among the different optimization algorithms compared in Tab. 1, the proposed OOA-PI (Osprey Optimization Algorithm with PI controller) stands out as the most efficient, with a remarkable efficiency of 98.6%. Compared to traditional algorithms like P&O, the OOA-PI algorithm demonstrates a significant improvement in efficiency. The algorithm optimizes the values of the controller parameters (K_p and K_i) using the OAA, which mimics the hunting behavior of ospreys. This allows the algorithm to adaptively tune the controller to achieve better control of the system.

Table 1 Performance analysis of proposed system

S. No	Methods	Efficiency / %
1	P&O	81%
2	FUZZY	86%
3	ANFIS	93%
4	PSO-PI	95%
5	OOA-PI	98.6%

Fig. 8 provides a comparison of the simulated output gains of various converters. Notably, the SEPIC converter exhibits the highest voltage gain among the tested converters, with a value of 2.5. This performance surpasses that of other converters, including Boost and Buck-Boost converters, which have gains within the range of 1.5. The CUK converter, on the other hand, achieves a gain of 2.

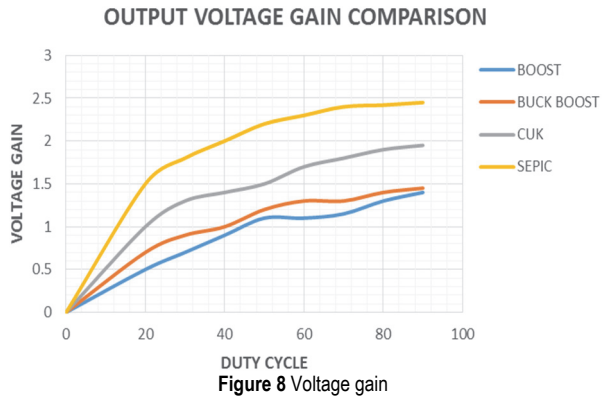

Figure 8 Voltage gain

Fig. 9 and Fig. 10 depict the comparison of THD values for the traditional and optimized PI controllers. The results indicate that the conventional PI controller yields a THD value of 3.8%, whereas the optimized PI controller achieves a lower THD value of 2.1%.

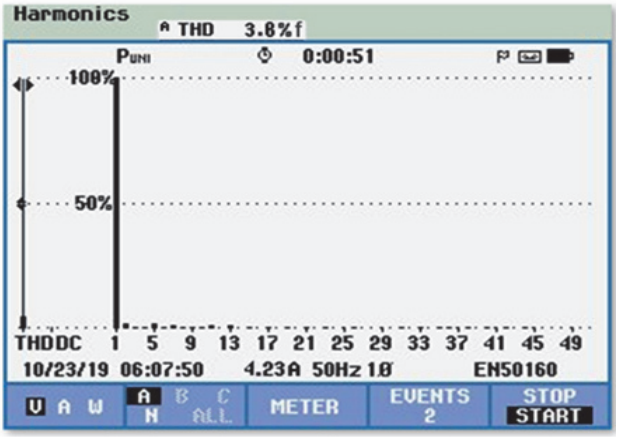

Figure 9 PI controller based THD

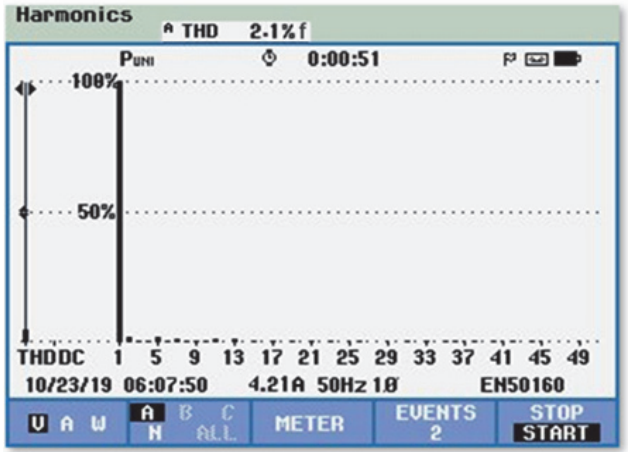

Figure 10 Optimized OOA + PI based THD

To evaluate the performance of the proposed system, both simulation and laboratory-scale experimentation were conducted. In the simulation environment, the irradiation level was manually adjusted at 0.1 seconds, while the temperature was maintained at a constant value of 250 degrees. This allowed for monitoring the corresponding changes in the converter and controller performance. In terms of dynamic behavior, the load was altered at 0.25 seconds to assess the system's response. In the laboratory-scale setup, the insolation level was not manually changed as the unpredictable environment was deemed representative. The proposed Single-Ended Primary Inductor Converter (SEPIC) and control system ensure a continuous flow of current from PV arrays. This directly translates into increased energy production and efficiency in PV systems deployed in smart grids.

5 CONCLUSION

This paper presented a PV based distribution system incorporating a SEPIC converter. Firstly, it effectively extracted the maximum power from the PV source by employing the OOA algorithm, outperforming other optimization algorithms. Additionally, the SEPIC converter minimized voltage ripples, ensuring a stable power output. The PI controller-based grid synchronization resulted in a reduced THD in the grid current. Furthermore, the voltage source inverter (VSI) complied with the harmonic's standards specified by IEEE, contributing to improved power quality. Comparative analysis revealed that the OOA-based SEPIC converter exhibited superior performance compared to PSO and ANFIS controllers. Moreover, it proved to be highly effective in compensating reactive power in the power grid. The system's performance was evaluated through MATLAB simulation and implementation using the DSPIC30F2010 controller. Overall, the proposed system offers enhanced performance, efficiency, and power quality, making it a promising solution for photovoltaic-based distribution systems.

REFERENCES

[1] Abdurazaq, E. & Muhammet, T. (2021). Algorithms to Model and Optimize a Stand-Alone Photovoltaic-Diesel-Battery System: An Application in Rural Libya. *Technical Gazette*, *28*(2), 523-529.

https://doi.org/10.17559/TV-20200530094834
[2] Kurtz, S., Ingrid, R., Wyatt, K. M., Pierre, J. V., Susan, H., Stuart, B., Ian, T., Keith, E.t, Lawrence, L. K., & Dean, L. (2018). Historical Analysis of Champion Photovoltaic Module Efficiencies. *IEEE J. Photovoltaics*, *8*(2), 363-372. https://doi.org/10.1109/JPHOTOV.2018.2794387
[3] Benda, V. (2015). Photovoltaics towards terawatts - progress in photovoltaic cells and modules. *IET Power Electron*, *8*(12), 2343-2351. https://doi.org/10.1049/iet-pel.2015.0102
[4] Song, S., Chen, G., Liu, Y., Hu, Y., Ni, K., & Wang, Y. (2020). A three-switch-based single-input dual-output converter with simultaneous boost & buck voltage conversion. *IEEE Trans. Ind. Informat*, *16*(7), 4468-4477. http://dx.doi.org/10.1109/TII.2019.2944872
[5] Seo, S. W., Ryu, J. H., Kim, Y., & Lee, J. B. (2021). Ultra-high step-up interleaved converter with low voltage stress. *IEEE Access*, *9*, 37167-37178. https://doi.org/10.1109/ACCESS.2021.3061934
[6] Yu, D., Yang, J., Xu, R., Xia, Z., Iu, H. H. C., & Fernando, T. (2018). A family of module-integrated high step-up converters with dual coupled inductors. *IEEE Access*, *6*, 16256-16266. https://doi.org/10.1109/ACCESS.2018.2815148
[7] Palanivel, M., Kaithmalai, U., & Parthasarathi, P. (2020). Comparative Analysis of Intelligent Controller Based MPPT for Photovoltaic System with Super Lift Boost Converter. *Technical Gazette*, *27*(2), 589-596. https://doi.org/10.17559/TV-20171029140308
[8] Wang, C., Li, M., Ouyang, Z., & Wang, G. (2021). Resonant push–pull converter with flyback regulator for MHz high step-up power conversion. *IEEE Trans. Ind. Electron*, *68*(2), 1178-1187. https://doi.org/10.1109/tie.2020.2969109
[9] Mohammadian, N. & Yazdani, M. R. (2018). Half-bridge flyback converter with lossless passive snubber and interleaved technique. *IET Power Electron*, *11*(2), 239-245. https://doi.org/10.1049/iet-pel.2017.0360
[10] Tseng, K., Huang, H., & Cheng, C. (2021). Integrated boost-forward-flyback converter with high step-up for green energy power-conversion applications. *IET Power Electron*, *14*(6), 27-37. https://doi.org/10.1049/pel2.12003
[11] Veerachary, M. (2005). Power tracking for nonlinear PV sources with coupled inductor SEPIC converter. *IEEE Transactions on Aerospace and Electronic Systems*, *41*(3), 1019-1029. https://doi.org/10.1109/TAES.2005.1541446
[12] Killi, M. & Samanta, S. (2015). An Adaptive Voltage-Sensor-Based MPPT for Photovoltaic Systems With SEPIC Converter Including Steady-State and Drift Analysis. *IEEE Transactions on Industrial Electronics*, *62*(12), 7609-7619. https://doi.org/10.1109/TIE.2015.2458298
[13] Paul, R., Bhattacharya, A., & Chatterjee, K. (2022). A Novel SEPIC-Ćuk Based High Gain Solar PV Micro-Inverter for Grid Integration. *IEEE Transactions on Industrial Electronics.* https://doi.org/10.1109/TIE.2022.3232655
[14] Chiang, S. J., Shieh, H. J., & Chen, M. C. (2009). Modeling and Control of PV Charger System With SEPIC Converter. *In IEEE Transactions on Industrial Electronics*, *56*(11), 4344-4353. https://doi.org/10.1109/TIE.2008.2005144
[15] Mamarelis, E., Petrone, G., & Spagnuolo, G. (2014). Design of a Sliding-Mode-Controlled SEPIC for PV MPPT Applications. *IEEE Transactions on Industrial Electronics*, *61*(7), 3387-3398. https://doi.org/10.1109/TIE.2013.2279361
[16] Balakishan, P.,Chidambaram, I. A., & Manikandan, M. (2023). An ANN Based MPPT for Power Monitoring in Smart Grid using Interleaved Boost Converter. *Technical Gazette*, *30*(2), 381-389. https://doi.org/10.17559/TV-20220820194302
[17] Soon, T. K. & Mekhilef, S. (2015). A Fast-Converging MPPT Technique for Photovoltaic System Under Fast-Varying Solar Irradiation and Load Resistance. *IEEE Transactions on Industrial Informatics*, *11*(1), 176-186. https://doi.org/ 10.1109/TII.2014.2378231.
[18] Darwish, A., Massoud, A. M., Holliday, D., Ahmed, S., & Williams, B. W. (2016). Single-Stage Three-Phase Differential-Mode Buck-Boost Inverters With Continuous Input Current for PV Applications. *IEEE Transactions on Power Electronics*, *31*(12), 8218-8236. https://doi.org/10.1109/TPEL.2016.2516255
[19] Poovizhi, M., Senthil Kumaran, M., Anitha, R. J., & Murugesan, K. (2022). An optimized design modelling of PV integrated SEPIC-based four-switch inverter for sensorless PMBLDC motor control. *Automatika*, *63*(1), 1560-1566. https://doi.org/10.1080/00051144.2021.2008621
[20] Singh, K., Badoni, M., & Tatte, Y. N. (2020). A Multifunctional Solar PV and Grid Based On-Board Converter for Electric Vehicles. *IEEE Transactions on Vehicular Technology*, *69*(4), 3717-3727. https://doi.org/10.1109/TVT.2020.2971971
[21] Mohammed, K. K., Mekhilef, S., & Buyamin, S. (2022). Improved Rat Swarm Optimizer Algorithm-based MPPT under partially shaded conditions and load variation for PV systems. *IEEE Transactions on Sustainable Energy.* https://doi.org/10.1109/TSTE.2022.3233112
[22] Hasanpour, S., Nouri, T., Blaabjerg, F., & Siwakoti, Y. P. (2023). High Step-Up SEPIC-Based Trans-Inverse DC–DC Converter With Quasi-Resonance Operation for Renewable Energy Applications. *IEEE Transactions on Industrial Electronics*, *70*(1), 485-497. https://doi.org/10.1109/TIE.2022.3150103
[23] Nathan, K., Ghosh, S., Siwakoti, Y., & Long, T. (2019). A New DC–DC Converter for Photovoltaic Systems: Coupled-Inductors Combined Cuk-SEPIC Converter. *IEEE Transactions on Energy Conversion*, *34*(1), 191-201. https://doi.org/10.1109/TEC.2018.2876454

Contact information:

Ravikumar SUDHANTHIRARAJAN, Research Scholar
(Corresponding author)
Department of Electrical and Electronics Engineering,
St. Michael College of Engineering, Sivagangai, Tamilnadu
E-mail: kumar.p.s@outlook.com; vmrk2024@gmail.com

Venkatanarayanan SUBARAMANIYAN, Professor
Department of Electrical and Electronics Engineering,
KLN College of Engineering, Sivagangai, Tamilnadu
E-mail: venjeyeee@gmail.com